D. BOCHENEK[1]*, K. OSIŃSKA[1], M. MANKIEWICZ[1], P. NIEMIEC[1], G. DERCZ[1]

TECHNOLOGY AND DIELECTRIC PROPERTIES OF THE KNLN DOPED WITH Nd^{3+} AND Pr^{3+} IONS

The paper presents the technology and basic properties of three compositions of lead-free ceramics: (i) $(K_{0.44}Na_{0.52}Li_{0.04})NbO_3$, (ii) $(K_{0.44}Na_{0.52}Li_{0.04})NbO_3+0.5\%mol\ Nd_2O_3$ and (iii) $(K_{0.44}Na_{0.52}Li_{0.04})NbO_3+0.5\%mol\ Pr_2O_3$. Powders of the designed compositions based on KNLN were obtained with the classic ceramic technology, as a result of solid phase synthesis, from a mixture of simple oxides and carbonates. The synthesis of ceramic powders was carried out at $T_s = 900°C$ for $t_s = 4$ h, while compaction by free sintering at $T_{sint} = 1100°C$ for $t_{sint} = 2$ h.

XRD studies have shown that doping with praseodymium and neodymium promotes the formation of the tetragonal phase in the base composition $(K_{0.44}Na_{0.52}Li_{0.04})NbO_3$ at lower temperatures. On the other hand, microstructural tests have shown that the admixture of neodymium and praseodymium improves the sinterability of ceramic samples during the technological process; however, the ceramic samples still exhibit high porosity.

Keywords: lead free ceramics, sodium potassium niobate, ferroelectrics, doped

1. Introduction

For many years, the solid solution of lead zirconate and lead titanate (PZT) has been the main material used in the construction of piezoelectric sensors and transducers in microelectronics. The ability to modify the basic chemical composition of PZT, as well as developed and properly carried out technology, allows the production of ceramic materials for specific applications in microelectronics [1-3,4]. Multicomponent PZT is the most widely used piezoelectric due to the very good piezoelectric properties thereof (especially for compositions from the morphotropic area). Despite the undeniable advantages of PZT ceramics, it cannot be ignored that it contains a significant amount of lead (even above 60% by weight). Also, the evaporation of PbO during technological processes and the difficulty of recycling and utilizing this type of ceramic materials has a negative impact on the environment and is a serious threat to the health of humans and animals [1-2,5]. All these negative phenomena cause the need to search for new lead-free ferroelectric materials with functional properties similar to the widely used PZT, which will be an alternative thereof [6-7].

In recent years, many attempts have been made to design and develop lead-free ceramic technology, e.g. $BaTiO_3$ (BT), $Bi_{0.5}Na_{0.5}TiO_3$ (BNT), $(K_{0.5}Bi_{0.5})TiO_3$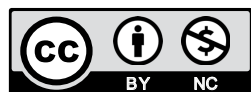 (KBT), $BaFe_{0.5}Nb_{0.5}O_3$ (BFN) or $BiFeO_3$ (BFO) [1,8-13]. However, low Curie temperatures of most of these materials and relatively poor dielectric and piezoelectric properties do not allow their commercial use in electronic devices and converters.

One of more promising ferroelectric materials as an alternative for PZT is sodium potassium niobate $(K,Na)NbO_3$ (KNN). This material is characterized by high Curie temperature and good piezo- and ferroelectric properties. Currently, a large interest in KNN ceramics is observed, in the direction of increasing its application possibilities, i.e. improving sinterability (during the technological process), physical properties and stability of parameters [1-3]. At room temperature, sodium potassium niobate has an ABO_3 perovskite type crystal structure. Temperature dielectric tests of KNN ceramics indicate a number of phase transitions in this material [1,6]. At a temperature of about $T = 123°C$, there is a phase transition from the rhombohedral phase to the orthorombic phase, while at about $T = 200°C$, there is a phase transition from the orthorombic phase to the tetragonal phase. At the temperature of approx. $T = 420°C$, another phase transition takes place from the tetragonal phase to the regular para-electric phase.

However, despite the good properties of KNN, due to technological difficulties, it is currently not possible to use this ceramics on a large scale. The problem is high volatility of al-

kaline elements in the sintering process, low density of sintered samples and high hygroscopicity of the substrates used for the synthesis of ceramic powders in the solid phase [2-3,14]. Admixing KNN ceramics, even with small amounts of lithium Li^+ ions, can improve the sinterability of the material and can have a positive effect on the value of the optimal sintering temperature, thereby improving the dielectric properties of the material [15-18]. In order to improve the density of KNN ceramics, hot pressing of the sintering method can be used. However, the hot pressing method is quite expensive and – due to its specificity – is not used in the industry for high volume production [3].

The purpose of this work was to obtain lithium ion modified potassium niobate ceramics $(K_{0.44}Na_{0.52}Li_{0.04})NbO_3$ (KNLN) and two compositions doped with neodymium ions $(K_{0.44}Na_{0.52}Li_{0.04})$ $NbO_3 + 0.5\%mol\ Nd_2O_3$ (KNLN:Nd) and praseodymium ions $(K_{0.44}Na_{0.52}Li_{0.04})NbO_3 + 0.5\%mol\ Pr_2O_3$ (KNLN:Pr), as well as determine the effect of the admixtures used on the properties of the obtained ceramic materials.

2. Experiment

KNLN powders were made with the classic ceramic technology, as a result of solid phase synthesis, from a mixture of simple oxides and carbonates according to the reaction equation:

$$0.22K_2CO_3 + 0.26Na_2CO_3 + 0.02Li_2CO_3 +$$
$$+ 0.5Nb_2O_5 \rightarrow (K_{0.44}Na_{0.52}Li_{0.04})NbO_3 + 0.5CO_2\uparrow.$$
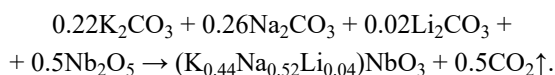
Potassium carbonate K_2CO_3 (POCH, 99.99%), sodium carbonate Na_2CO_3 (Sigma-Aldrich, 99.5%), lithium carbonate Li_2CO_3 (Sigma-Aldrich 99.0%) and niobium oxide Nb_2O_5 (Alfa Aesar 99.5%) were used as reaction substrates. The basic composition of KNLN ceramics was molar doped with neodymium oxides Nd_2O_3 (Sigma-Aldrich 99.9%) and praseodymium Pr_2O_3 (Aldrich, 99.99%) in the amount of 0.5%mol (KNLN + 0.5%mol Nd_2O_3, KNLN + 0.5%mol Pr_2O_3). The admixtures used for the base composition were introduced at the stage of mixing powders before synthesis. The stoichiometric mixture of substrate powders, with the addition of ethyl alcohol (POCH, 99.99%), was mixed for $t = 24$ h in a planetary mill (zirconium yttrium grinders 3Y-TZP). After mixing, the powders were dried and then the dry powders were molded and synthesized at $T = 900°C$ for $t = 4$ h. In the next stage, the synthesized ceramic samples were cleaned of Al_2O_3, crushed and milled again in a planetary mill for $t = 24$ h, with the addition of ethyl alcohol. After mixing, the powders were air-dried and formed into pellets with a diameter of $d = 10$ mm, on a hydraulic press, at a pressure of $p = 120$ MPa. Compaction was carried out by the free sintering method under the conditions: $T = 1100°C$ for $t = 2$ h, with a temperature increase of 5°C/min.

The X-ray research at room temperature of the crystal structure was performed using a Philips X'Pert diffractometer. The microstructure and EDS (Energy Dispersive Spectrometry) study have been conducted with a JEOL JSM-7100F TTL LV Field Emission Scanning Electron Microscope. Temperature dielectric

measurements were made using a QuadTech 1920 Precision LCR Meter for a heating cycle (heating rate of 0.5°/min, frequencies of the measurement field from $v = 20$ Hz to 100 kHz), in the temperature range from 20°C to 600°C.

3. Results and discussion

For the obtained ceramic samples, density, porosity and water absorption were determined (Fig. 1) with the Archimedes method. Analysis of the obtained compositions showed that the added admixtures did not improve the density of the final ceramic product. The porosity and water absorption thereof also increase.
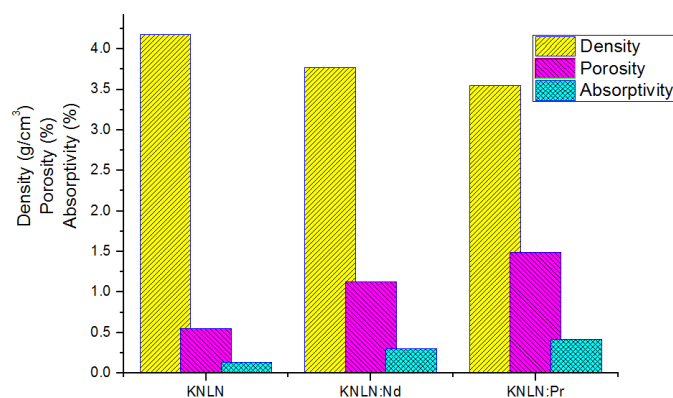

Fig. 1. Density, porosity and absorptivity of the ceramic samples

Fig. 2(a) shows the results of the XRD tests of the KNLN-type ceramic samples. In order to determine lattice parameter samples, X-ray diffraction patterns were fitted using the Rietveld method. The XRD measurements performed at room temperature (RT) showed that all ceramic compounds have a perovskite structure. On this basis, crystal structures can be approximately identified from the relative intensity (I) of the (002) and (200) diffraction peaks, whose I(002)/I(200) are 2:1 and 1:2 for the orthorhombic and tetragonal symmetry, respectively [19-20].

The XRD patterns (in the magnification i.e. in the range of 2θ from 44° to 48°) are presented in Fig. 2b. In the case of the undoped KNKN sample, the XRD patterns show a clearly visible (002)/(200) peak splitting in the proportion of 2:1, that confirming the orthorhombic symmetry. The best fit was done for the JCPDS 01-081-8642 pattern with space group Bmm2 ($\alpha = \beta = \gamma = 90°$, $a_0 = 5.6560$ Å, $b_0 = 3.9340$ Å, $c_0 = 5.6220$ Å). Doping of praseodymium and neodymium promotes the formation of the tetragonal phase in the base composition (KNLN) at lower temperatures. In the case of the KNLN:Nd and KNLN:Pr samples, the XRD patterns show a reflection disorder in the above 2θ range, and the coexistence of two phases (orthorhombic and tetragonal symmetries) is observed. In the case of the KNLN:Nd and KNLN:Pr samples, the XRD patterns show a reflection disorder in the above 2θ range, and the coexistence of two phases (orthorhombic and tetragonal symmetries) is observed. In the case of orthorhombic symmetry, the best fit was done for the JCPDS 01-081-8642 pattern (like in case KNLN
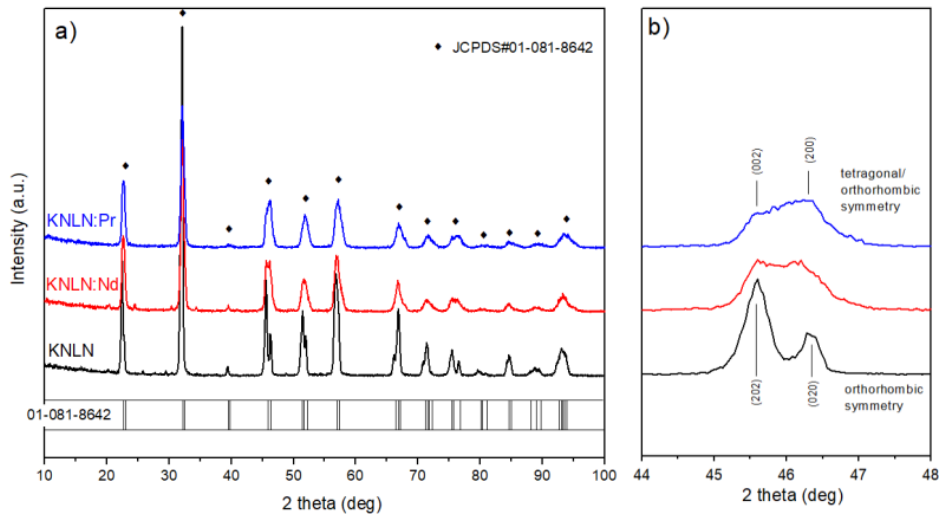
Fig. 2. XRD patterns of the KNLN, KNLN:Nd and KNLN:Pr materials

sample), while in the case of the second phase pattern of the tetragonal symmetry was fit (JCPDS 01-082-3272) with space group P4mm ($\alpha = \beta = \gamma = 90°$, $a_0 = 3.9564$ Å, $b_0 = 3.9564$ Å, $c_0 = 4.0376$ Å) [1].

Fig. 3 presents the SEM microstructural images of the fractures of the obtained ceramic samples. In the case of the undoped KNLN composition (Fig. 3a), the microstructure is characterized by a large grain with a characteristic cube shape. Cubic grains have clearly visible grain boundaries. The average grain size is 1.87 µm. In the case of KNLN doped with neodymium (Fig. 3b) and praseodymium (Fig. 3c), while maintaining the

same technological conditions, a greater degree of grain refinement is observed, as compared to pure KNLN. The microstructure is formed by fine ceramic grains of irregular shape which are strongly grown together. The admixture of neodymium and praseodymium introduced into KNLN improves sinterability during the technological process, and the microstructure shows less porosity in comparison with the undoped KNLN sample.

The lead-free ceramic material was subjected to the EDS homogeneity testing (Fig. 4). The EDS analysis was carried out from 5 random areas of the sample surfaces. The EDS analysis of the element distribution confirmed the qualitative chemical
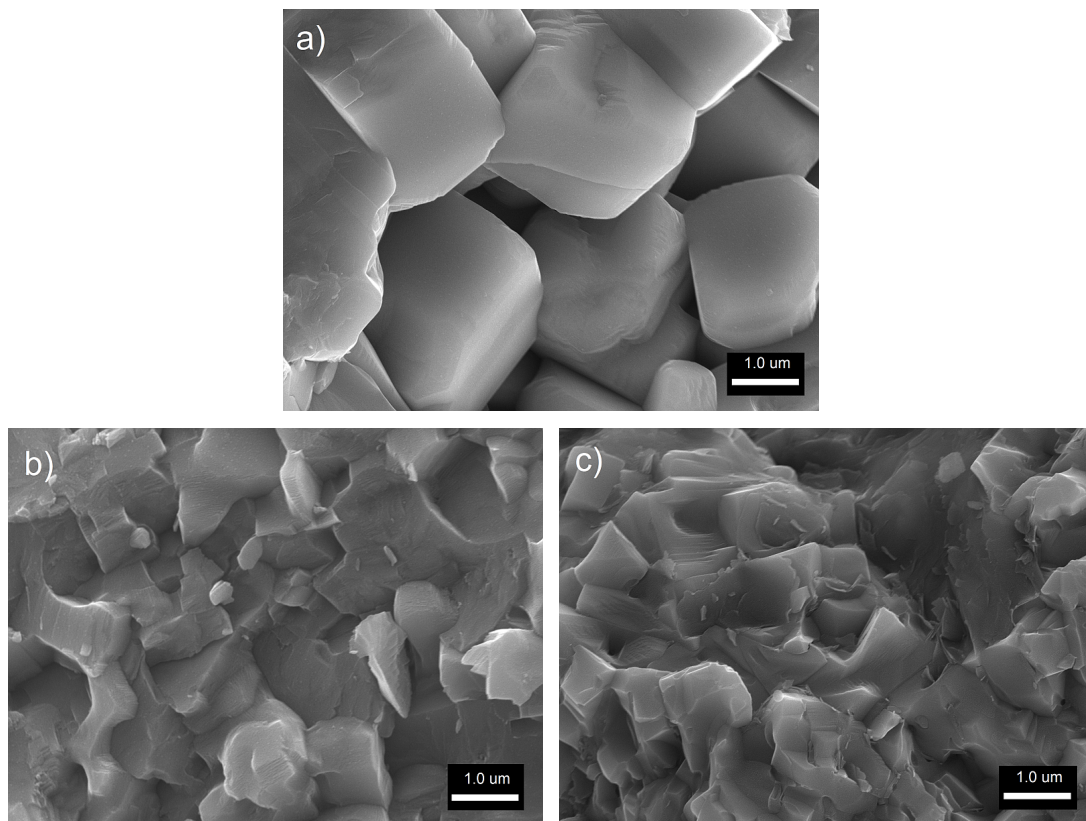

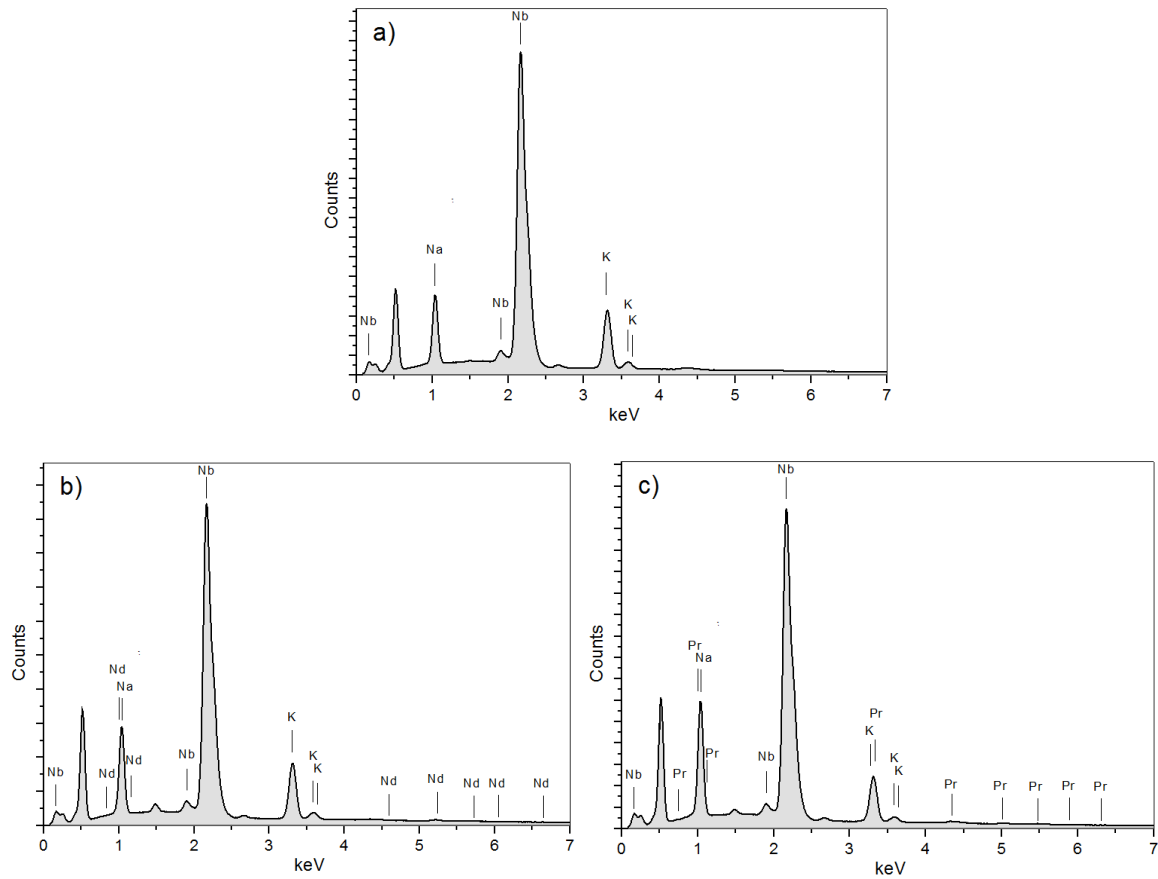Fig. 3. SEM images of the KNLN (a), KNLN:Nd (b) and KNLN:Pr (c) materials

Fig. 4. EDS tests of the (a) KNLN, (b) KNLN:Nd and (c) KNLN:Pr materials

composition of the designed ceramic materials. Compared to theoretical calculations, sodium deficiency and a small excess of potassium and niobium are observed in the case of the KNLN sample. A similar trend occurs for the doped compositions. In the case of the sample doped by neodymium (KNLN:Nd), also a small excess of neodymium are observed, while in case of the sample doped by praseodymium (KNLN:Pr), theoretical and experimental results are almost identical. All deviations from the initial composition are within an acceptable range. Theoretical and experimental percentages of elements (expressed as oxides) of KNLN-type ceramic samples are given in Table 1.

KNLN, KNLN:Nd and KNLN:Pr, respectively. The reason for the decrease in electrical resistivity at room temperature of the KNLN:Nd and KNLN:Pr samples is the introduction of Nd^{3+} and Pr^{3+} admixtures into the base composition. Considering the ionic radii of admixtures of neodymium r_{Nd} = 98.3 pm (CN = 6) and praseodymium r_{Pr} = 99 pm (CN = 6), they will substitute for the potassium K^+ (r_K = 138 pm, CN = 6) and sodium Na^+ (r_{Na} = 102 pm, CN = 6) in the KNLN base composition. This

TABLE 1

Theoretical and experimental percentages of elements of KNLN type ceramics

Oxide formula	KNLN		KNLN:Nd		KNLN:Pr	
	Theoret. (%)	Exper. (%)	Theoret. (%)	Exper. (%)	Theoret. (%)	Exper. (%)
K_2O	12.17	12.42	12.05	12.15	12.05	12.62
Na_2O	9.46	9.28	9.37	8.94	9.37	9.86
Nb_2O_5	78.02	78.30	77.26	77.82	77.27	77.56
Li_2CO_3	0.35	—	0.35	—	0.35	—
Nd_2O_3	—	—	0.98	1.09	—	—
Pr_2O_3	—	—	—	—	0.96	0.95

At room temperature, the electrical resistivity of the ceramic samples are $3.2 \times 10^6\ \Omega m^{-1}$, $3.6 \times 10^4\ \Omega m^{-1}$ and $1.1 \times 10^4\ \Omega m^{-1}$ for
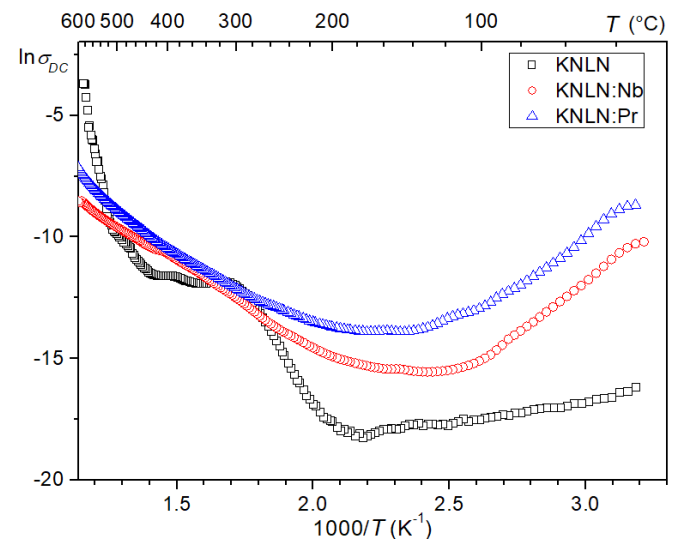

Fig. 5 The $\ln \sigma_{DC}(1/T)$ relationship for the KNLN type materials

type of substitution with excess valence in materials with a perovskite structure decreases the Curie T_C temperature, however increases dielectric loss and electrical conductivity at lower temperatures. This is also confirmed by the above-mentioned dielectric properties study.

In Fig. 5, the $\ln\sigma_{DC}$ versus $1000/T$ dependence of the PNLN-type ceramics are presented. In the case of the KNLN

ceramics, there are a few changes as a curve on the plot. They are associated with the occurring phase transitions into the obtained material, which was also confirmed by temperature dielectric tests (Fig. 6). In the case of the doped ceramic samples, there is one good visible inflexion on the curves, as well as no apparent change in the slope of the curve around the phase transition temperature.
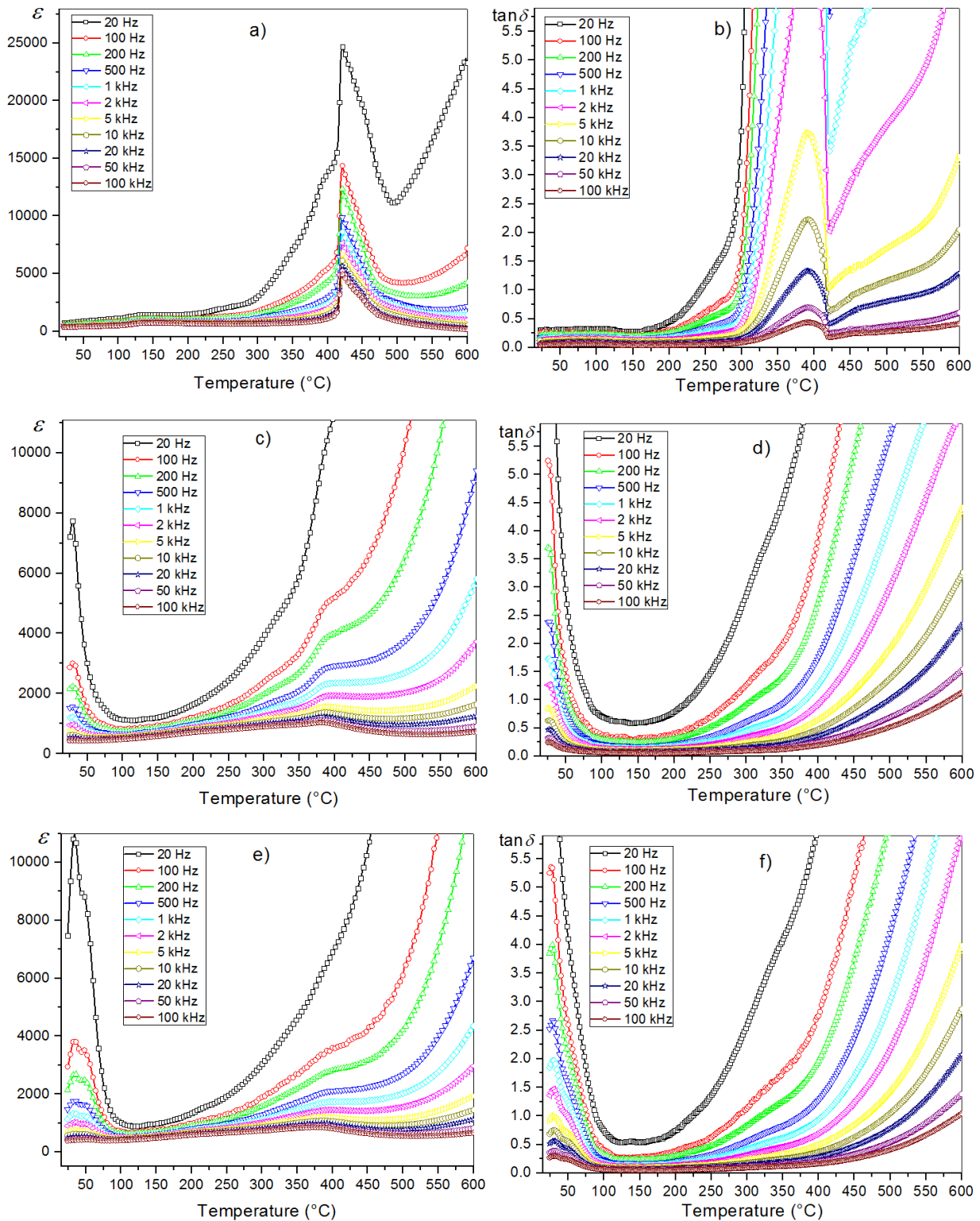

Fig. 6. Temperature dependence of $\varepsilon(T)$ (Fig. 6a, c, e) and $\tan\delta(T)$ (Fig. 6b, d, f) for the KNLN type materials (heating cycle). Fig. 6a,b for KNLN sample, Fig. 6c, d for KNLN:Nb sample and Fig. 6e, f for KNLN:Pr sample

TABLE 2

Electrophysical parameters of the lead free KNLN-type materials

	KNLN	KNLN:Nb	KNLN:Pr
ρ (g/cm^3)	4.18	3.77	3.55
T_{O-T}/T_{T-C} (°C) [1]	149/421	- /393	- /394
ε at RT [1]	426	1193	1138
ε at T_{O-T}/T_{T-C} [1]	907/8633	- /2337	- /1722
$\tan\delta$ at RT [1]	0.151	1.72	1.84
ρ_{DC} (Ωm^{-1})	3.2×10^6	3.6×10^4	1.1×10^4

RT – room temperature, [1] – test at 1 kHz

Temperature tests of the dielectric properties of KNLN-type ceramics are presented in Fig. 6 (Fig. 6a, b for KNLN sample, Fig. 6c, d for KNLN:Nb sample and Fig. 6e, f for KNLN:Pr sample). In the case of the tests of the non-doped composition of KNLN at temperature $\varepsilon(T)$, they confirmed the occurrence of several maxima associated with the occurring phase transformations in the tested material (Fig. 6a). The first maximum is out of focus and heavily blurred. It occurs at T_{O-T} = 149°C and is associated with the phase transition from the orthorhombic phase to the tetragonal phase. At the temperature course $\varepsilon(T)$, at the temperature T_{T-C} = 421°C, there is also a sharp phase transition (first type) from the ferroelectric (tetragonal) phase to the regular paraelectric phase. The maximum value of electric permittivity at the phase transition point (T_{T-C}) is 8633. Temperature tests of dielectric loss are shown in Fig. 6b. Up to about 200°C, dielectric loss occurs at a constant level and then starts to increase. Above 300°C, the increase is rapid, which is associated with a large increase in electric conductivity at higher temperatures.

In the case of doped compositions, the $T-C$ phase transition becomes very blurred, and the maximum temperature T_{T-C} shifts towards the lower temperature. Dielectric loss for these compositions does not increase as rapidly as for the undoped KNLN composition, however exhibits higher values at room temperature.

4. Conclusion

The paper presents the technology and basic properties of three compositions of lead-free ceramics: (i) $(K_{0.44}Na_{0.52}Li_{0.04})NbO_3$, (ii) $(K_{0.44}Na_{0.52}Li_{0.04})NbO_3$ + 0.5%mol Nd_2O_3 and (iii) $(K_{0.44}Na_{0.52}Li_{0.04})NbO_3$ + 0.5%mol Pr_2O_3. The studies have shown that doping of praseodymium and neodymium promotes the formation of the tetragonal phase in the KNLN base composition at lower temperatures. On the other hand, microstructural tests have shown that the admixture of neodymium and praseodymium improves the sinterability of ceramic samples during the technological process. However, the obtained ceramic materials still show high porosity, which significantly limits their applicability.

Since KNLN material is an extremely promising lead-free material in the aspect of replacing lead materials obtained on the basis of PZT, it is advisable to further explore and improve the existing ceramic technologies, as well as to search for new technologies and techniques that will ensure obtaining dense ceramic samples showing optimal performance parameters. Obtaining a material with a dense non-porous structure guarantees its optimal and stable electrophysical parameters and properties. In order to further improve the physical properties of the KNLN-based material, the amount of praseodymium and neodymium admixture introduced into KNLN can be changed. Multi-component doping may also be done. The aforementioned works will be the subject of the next research of the authors of this publication.

REFERENCES

[1] Z.-X. Xu, J.-M. Yan, L. Guo, M. Xu, F.-F. Wang, Y.-K. Liu, R.-K. Zheng, J. Mater. Sci.-Mater. El. **29**, 2, 1341-1348 (2018).

[2] Y. Zhao, Z. Xu, H. Li, J. Hao, J. Du, R. Chu, D. Wei, G. Li, J. Electron. Mater. **46** (1) 116-122 (2017).

[3] Y. Zhao, J. Du, X. Niu, J. Hao, W. Li, P. Fu, Z.-J. Xu, J. Mater. Sci.-Mater. El. **29**, 6. 4791-4800 (2018).

[4] J.A. Bartkowska, J. Magn. Magn. Mater. **374**, 703-706 (2015).

[5] J. Portelles, N. Palmero, J. Fuentes, R. López Noda, O. Raymond Herrera, M. P. Cruz, J. M. Siqueiros, J. Appl. Phys. **122**, 234102 (2017).

[6] R. Rai, R. Rani, S. Sharma, A. Kholikin, J. Alloy. Compd. **577**, 575-580 (2013).

[7] D. Bochenek, K. Osińska, P. Niemiec, M. Adamczyk, T. Goryczka, Adv. Appl. Ceram. **118**, 6, 351-359 (2019).

[8] L. Zhang, J. Wen, Z. Zhang, J. Yang, H. Huang, Q. Hu, H. Zhuang, H. Yu, Phys. B **560**, 155-161 (2019).

[9] M. Appiah, H. Hao, W. Chen, Ch. Chen, Z. Yao, M. Cao, H. Liu, J. Wuhan Univ. Technol. **33**, 3, 589-597 (2018).

[10] M. Xiao, H. Sun, Y. Wei, L. Li, P.D. Zhang, Mater. Sci.-Mater. El. **29**, 20, 17689-17694 (2018).

[11] S. Pattipaka, M. Peddigari, P. Dobbidi, Ceram. Int. **43**, S151-S157 (2017).

[12] P. Czaja, J. Suchanicz, D. Bochenek, G. Dercz, M. Piasecki, W. Hudy, Phase Transit. **91**, 1051-1059 (2018).

[13] D. Bochenek, P. Niemiec, A. Chrobak, G. Ziółkowski, A. Błachowski, Mater. Charact. **87**, 36-44 (2014).

[14] M.R. Saeri, A. Barzegar, H. Ahmadi Moghadam, Ceram. Int. **37**, 83083-3087 (2011).

[15] Y. Zhen, J.-F. Li, J. Am. Ceram. Soc. **89**, 12, 3669-3675 (2006).

[16] J. Andrejovska, J. Mihalik, J. Koval, V. Brunckova, H. Dusza, Acta Metallurgica Slovaca **15**, 2, 112-116 (2009).

[17] S. Wongsaenmai, S. Ananta, R. Yimnirun, Ceram. Internat. **38**, 1, 147-152 (2012).

[18] K. Osińska, D. Bochenek, K. Guzak, Materiały ceramiczne / Ceramic Materials/ **69**, 4, 359-363 (2017).

[19] Q. Li, M.H. Zhang, Z.X. Zhu, K. Wang, J.S. Zhou, F.Z. Yao, J.F. Li, J. Mater. Chem. C **5**, 549-556 (2017).

[20] B.H. Liu, P. Li, B. Shen, J.W. Zhai, Y. Zhang, F. Li, X. Liu, Ceram. Int. **43**, 8004-8009 (2017).